

복잡한 지반층을 고려한 지반-말뚝-구조물의 상호작용 동해석

Dynamic Analysis of Soil-Pile-Structure Interaction Considering a Complex Soil Profile

박장호¹⁾ · 박재균²⁾

Park, Jang-Ho · Park, Jaegyun

국문 요약 >> 지반-말뚝-구조의 상호작용을 정밀하게 해석하기 위해서는 토층, 말뚝 그리고 구조물의 적절한 묘사가 필요하다. 일반적으로 사용하는 유한요소해석의 경우에는 지반이나 구조물의 물성이 바뀌는 경계를 따라서 요소의 경계가 정해지게 된다. 그러나 실제로는 토층 단면과 말뚝의 형상이 매우 복잡하여 요소의 배열이 매우 어려운 작업이 될 수 있다. 이 어려움을 해결하기 위하여, 이 논문에서는 불연속선의 위치에 관계없이 규칙적인 요소를 사용하여 쉽게 적분을 가능하게 하는 다른 적분 방법을 채택하였다. 이 방법을 적용함으로써 요소는 매우 빠르고 규칙적인 강성 매트릭스를 만든다. 구조물 응답에 대한 토층과 말뚝의 영향을 조사하였고, 예를 통하여 본 방법의 유효성을 보였다. 탄성 말뚝의 사용으로 20% 대의 가속도 감소 효과를 얻었고 지반 층의 모양에 따라 그 영향이 변하는 것을 확인하였다.

주요어 지반-말뚝-구조물 상호작용, 물성 불연속성, 불연속 수치 적분, 복잡한 경계면

ABSTRACT >> The precise analysis of soil-pile-structure interaction requires a proper description of soil layer, pile, and structure. In commonly used finite element simulations, mesh boundaries should match the material discontinuity line. However, in practice, the geometry of soil profiles and piles may be so complex that mesh alignment becomes a wasteful and difficult task. To overcome these difficulties, a different integration method is adopted in this paper, which enables easy integration over a regular element with material discontinuity regardless of the location of the discontinuity line. By applying this integration method, the mesh can be generated rapidly and in a highly structured manner, leading to a very regular stiffness matrix. The influence of the shape of the soil profile and piles on the response is examined, and the validity of the proposed soil-pile structure interaction analysis method is demonstrated through several examples. It is seen that the proposed analysis method can be easily used on soil-pile-structure interaction problems with complex interfaces between materials to produce reliable results regardless of the material discontinuity line.

Key words Soil-pile-structure interaction, Material discontinuity, Numerical integration of discontinuity, Complicated interface

1. Introduction

Many construction sites may have soft soil layers with different material properties. When a structure is built on such a soft soil site, the geometry and property of the supporting soil exert larger influence on structural behavior. This effect is caused by the flexibility of the

supporting soil and soil-structure interaction. One of frequently used method to decrease the influence of soil-structure interaction is the installation of piles under the foundation of a structure. However, if the structure is massive, this method may cause soil-pile-structure interaction and the soil-pile-structure interaction may become an important consideration in the seismic design of structures.

Various soil-structure interaction analysis methods have been developed and are currently being applied to analyze various structures at soft soil sites.⁽¹⁻⁷⁾ Most of these methods utilize a simplified soil profile in their numerical algorithms. These simplified approximations, such as horizontally flat-layered soil, are mainly used to

¹⁾ 정회원·아주대학교 환경건설교통공학부, 부교수

²⁾ 정회원·단국대학교 토목환경공학과, 조교수

(교신저자: jpark@dankook.ac.kr)

본 논문에 대한 토의를 2009년 8월 30일까지 학회로 보내 주시면 그 결과를 게재하겠습니다.

(논문접수일 : 2008. 11. 6 / 수정일 1차 : 2009. 4. 5, 2차 : 2009. 5. 5 / 게재확정일 : 2009. 5. 6)

avoid the complexity of the geometry and distribution of interfaces between materials. However, these simplified approaches cannot consider the characteristics of soil, pile, and structure with complex interfaces correctly and reduce the reliability of the analysis. Other methods which try to describe complicated boundaries of materials exactly consume so much effort and time that those methods have limitations on three dimensional dynamic analyses.

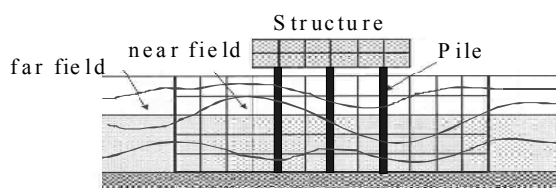
Generally one finite element can be endowed only with one material property. This makes it difficult to generate proper meshes when the interface between materials is complicated. Furthermore, it is likely that the finite element may be distorted and may lose its convexity, which leads to ill-conditioned stiffness matrix. This paper adopts a numerical integration method, which can rapidly calculate the stiffness of a finite element with material discontinuity.⁽⁸⁾ Application of the mentioned integration method to three dimensional soil-pile-structure interaction analysis can produce more accurate results on the dynamic behavior of soil-pile-structure systems. This method also offers advantages such as the rapid mesh generation of three-dimensional soil-pile-structure systems with complicate interfaces and the elimination of element distortion.

2. Analysis method of soil-pile-structure interaction

The proposed analysis method consists of a scheme for the numerical integration of a discontinuous function and an analysis method of a soil-structure interaction system.

2.1 Numerical integration scheme of a discontinuous function

In case of ordinary finite element analysis for a



〈Fig. 1〉 Soil-Pile-Structure System

structure with various materials, the interface between materials is used as an element boundary to avoid material discontinuity in an element, which leads to an ordinary stiffness matrix. However, the modeling gets more difficult and the shape of the element is distorted resulting in an ill-conditioned stiffness matrix when the interface between materials is complicated.⁽⁹⁾

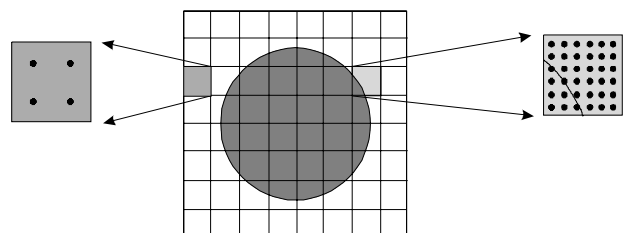
To overcome these shortcomings, this study adopts a different numerical integration method which can calculate more accurately the stiffness and mass matrices of an element with material discontinuity. Fig. 2 presents a solid consisting of two different materials. The application of a structured mesh to the solid leads to finite elements with one or two materials. The numerical integration for an element consisting of a unique material is trivial, but the integration for an element composed of two materials is more delicate. The main concept of the different numerical integration method for an element with material discontinuity is to use appropriately increased number of Gauss quadrature points. Points in the magnified element in Fig. 2 represent Gauss quadrature points.

To simplify the scheme, let us consider a scalar function $f(\varsigma)$ in Fig. 3, which has a jump at $\varsigma = \delta$. This function can be considered as the sum of one continuous function $c(\varsigma)$ and unit step function part as

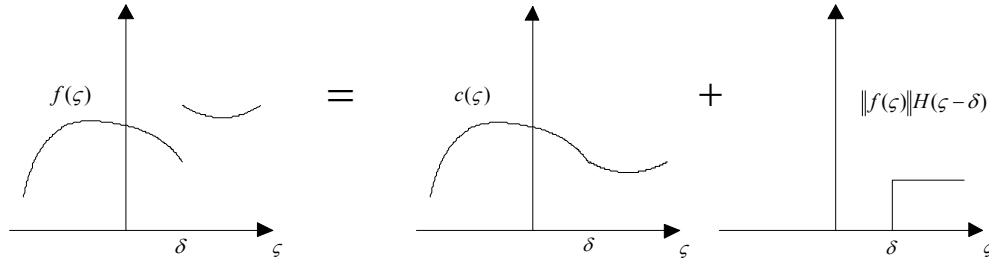
$$f(\varsigma) = c(\varsigma) + \|f(\delta)\| H(\varsigma - \delta) \quad (1)$$

where ς is the local coordinate, $H(\varsigma - \delta)$ is the unit step function, and $\|f\|$ is the jump operator which calculates the difference between left and right limit values of $f(\varsigma)$ on the point of discontinuity.

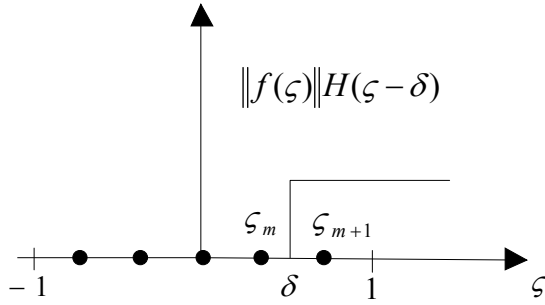
The integration of the discontinuous function $f(\varsigma)$ over a region leads to equation (2).



〈Fig. 2〉 Modeling of a solid composed of two different materials



〈Fig. 3〉 Separation of a discontinuous function



〈Fig. 4〉 Numerical integration of a jump function

$$\int_{-1}^1 f(\zeta) d\zeta = \int_{-1}^1 \{c(\zeta) + \|f(\delta)\|H(\zeta - \delta)\} d\zeta \quad (2)$$

Application of the one-dimensional Gauss quadrature rule to the above equation results in the error bounds of the above integration.⁽¹⁰⁾

$$\begin{aligned} \text{error} &= \left| \int_{-1}^1 f(\zeta) d\zeta - \left\{ \sum_{i=1}^N (c(\zeta_i) + \|f(\delta)\|H(\zeta_i - \delta)) w_i \right\} \right| \\ &= \|f(\delta)\| \left| (1 - \delta) - \sum_{i=m+1}^N 1 \cdot w_i \right| \\ &\leq \|f(\delta)\| \left| \sum_{i=m}^N w_i - \sum_{i=m+1}^N w_i \right| \\ &\leq \|f(\delta)\| \cdot \max |w_i| \end{aligned} \quad (3)$$

where N is the number of Gauss quadrature points, w_i is the weight of the i -th Gauss quadrature point, and ζ_i is the location of the i -th Gauss quadrature point. Therefore, the error range of the Gauss quadrature integration on a discontinuous function is decided by the largest quadrature weight w_i , which leads to the following equation.⁽⁴⁾

$$\text{error} \leq \max |w_i| \approx 5.07 N^{-1.82} \quad (4)$$

The same method can be applied to the calculation of

〈Table 1〉 Error bounds of the proposed integration method

| Gauss rule | Error bound |
|--------------------------|-------------|
| $3 \times 3 \times 3$ | 0.7167 |
| $5 \times 5 \times 5$ | 0.3538 |
| $7 \times 7 \times 7$ | 0.2041 |
| $9 \times 9 \times 9$ | 0.1331 |
| $11 \times 11 \times 11$ | 0.0937 |

stiffness and mass matrices in three-dimensional finite elements. The error bounds in the calculation of matrices of an element are estimated in table 1. The element stiffness with material discontinuity is calculated with enough precision using an adequate number of Gauss quadrature points.

2.2 Analysis method of a soil-structure interaction

When a structure is constructed on soft soil, the flexibility of the supporting soil and the soil-structure interaction exert larger influence on its behavior. Therefore, precise models of the structure and soil are essential to estimate the soil-structure interaction properly. Methods for soil-structure interaction analysis are mainly classified as direct method and substructure method according to the way to include the soil in their analyses.⁽¹¹⁾ This paper adopts a direct method^{(12),(13)}, which is widely used because of its simplicity and accuracy. The structure is simplified to show its overall response characteristics and the soil and pile are modeled by structured non-uniform mesh as shown in Fig. 5 to perform soil-pile-structure interaction analysis.

The treatment of seismic input and boundary conditions is also very important because it affects significantly the response of the supporting soil media and the structure. The lateral and base boundary conditions for the soil

domain are modeled using a modified Lysmer transmitting/absorbing boundary such that the domain beyond the soil media of interest is replaced with a set of viscous dampers normal and tangential to the soil boundaries, since damping force is proportional to the wave velocity.⁽¹⁴⁾ On each node at the boundary, the tangential dashpot absorbs the energy of the shear wave and the normal dashpot absorbs the energy of the P-wave, as expressed by the following relations.

$$c_t = A\rho v_s \quad (5)$$

$$c_n = A\rho v_p \quad (6)$$

where ρ, v_p, v_s are respectively the soil density, P-wave velocity, and shear wave velocity. A represents the effective area. Generally the boundary effect reduces as the soil media gets larger.

3. Dynamic analysis of soil-pile-structure system with complicated interfaces

By the proposed method, three-dimensional soil-pile-structure systems are analyzed considering complicated interfaces between materials. The influence of soil profile and piles on the response is examined.

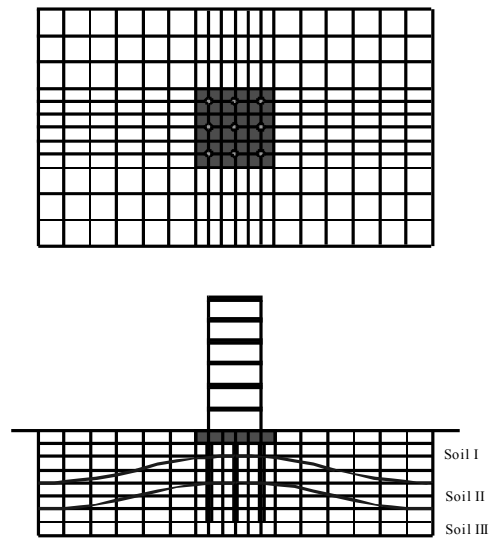
3.1 Structure and soil profile

In this paper, the soil-pile-structure interaction analysis was conducted on 7-story structures built on soft soil. The structure was modeled as illustrated in Fig. 5 with the properties summarized in Table 2. Floor B1 is located below the ground surface. The damping ratio of the structure model is assumed to be 0.03.

Dynamic analyses are performed on five different soil profiles. Soil profile nn stands for conventional soil profile model with horizontal flat layers. The other 4 cases (*mm*, *mp*, *pm*, *pp*) correspond to more realistic three-layered soft soils (Fig. 6) with uneven soil profiles expressed by sine and cosine functions. The soil is modeled as a rectangular parallelepiped with dimensions of 60m×36m×20m of which each direction is divided into 18×12×8 elements for a total of 1728 solid elements.

〈Table 2〉 Properties of structure model

| Floor | Level (m) | Stiffness (kN/m) | Mass (kg) |
|-------|-----------|------------------|-----------|
| 7 | 21.5 | - | 420000 |
| 6 | 18 | 3128000 | 420000 |
| 5 | 14.5 | 3416000 | 460000 |
| 4 | 11 | 3608000 | 460000 |
| 3 | 7.5 | 3956000 | 460000 |
| 2 | 4 | 4080000 | 460000 |
| 1 | 0 | 3416000 | 550000 |
| B1 | -3.5 | 10000000 | 700000 |

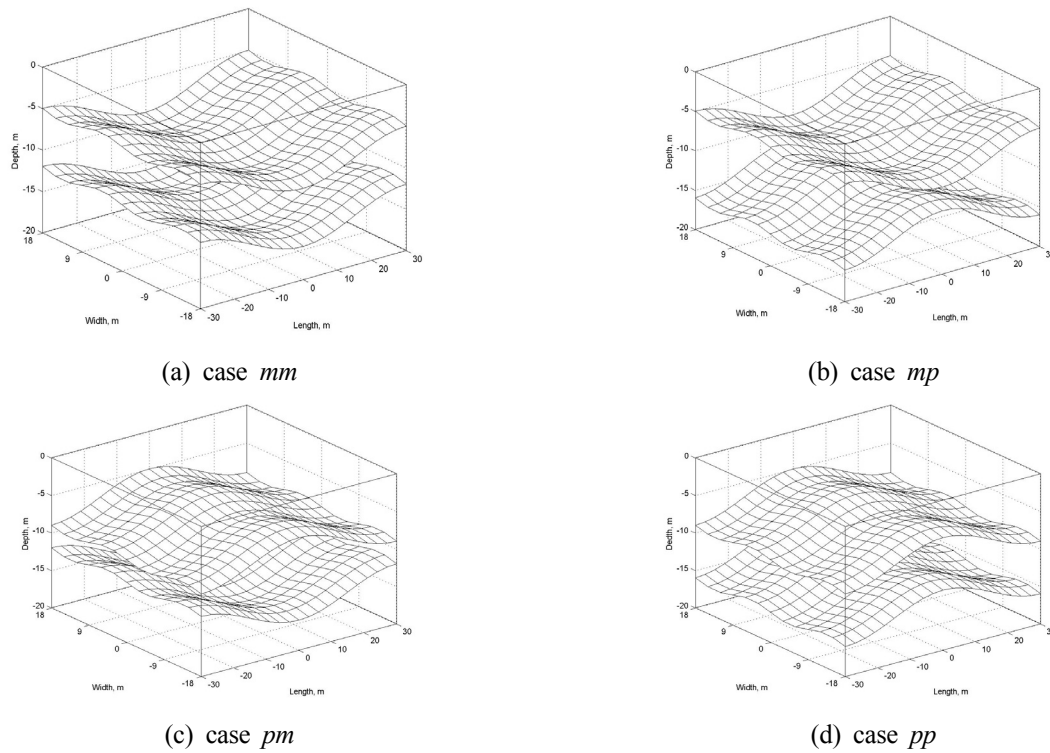


〈Fig. 5〉 Finite element model

The material properties of each soil layer are listed in table 3. Boundaries of vertical sides are modeled by tangential and normal dashpots, and the bottom surface is assumed to be in contact with the bedrock.

Piles are assumed to be linearly elastic with Young's modulus 19000MN/m², density 7850kg/m³, and Poisson's ratio 0.30. The radius of pile is 1.0m and all piles are modeled by finite elements embedded within structured mesh. This numerical experiment simply extends the validity of soil modeling in the paper⁽¹⁰⁾ to the case of general complex geometry of soil and piles such that piles are considered to be part of soil with different material property.

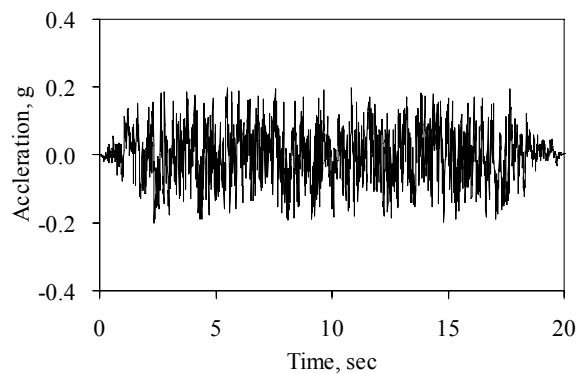
The artificial earthquake ground motion used as input acceleration at the bedrock has been generated based on the response spectrum prescribed in the Korean Highway Bridge Design Specifications⁽¹⁵⁾ (Fig. 7). According to a reference⁽¹⁶⁾, the PGA of this input is about 0.22g.



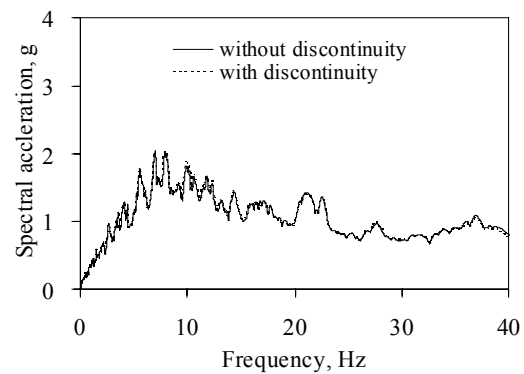
〈Fig. 6〉 Soil-Profiles

〈Table 3〉 Properties of the soil layers

| Layer (m) | S-wave velocity (m/s) | Density (kg/m ³) | Poisson's ratio | Damping ratio |
|-----------------|-----------------------|------------------------------|-----------------|---------------|
| Top (0-7.0m) | 300 | 1900 | 0.30 | 0.08 |
| Middle (-14.0m) | 650 | 2000 | 0.30 | 0.04 |
| Bottom (-18.0m) | 1000 | 2100 | 0.25 | 0.025 |



〈Fig. 7〉 Input ground motion at the bedrock (acceleration time history)



〈Fig. 8〉 free field motion with structured mesh(discontinuity) and unstructured mesh

3.2 Verification

To validate the proposed method, analyses of free field motion for soil profile case *mm* were performed. One model is divided by a structured mesh with discontinuity within an element and the other is divided along the surface of material discontinuity. Fig. 8 presents response spectra on the ground surface for both cases, which are in good agreement and proves the

validity of this method on the soil-structure interaction problem. Therefore, without loss of generality we can extend this method to the case of more than two material properties within one element.

3.3 Analysis results

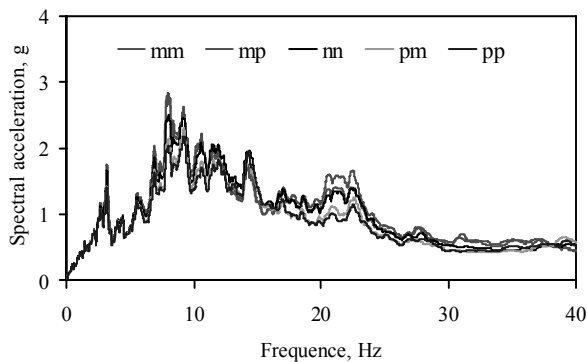
The proposed method has been applied to calculate the responses at the ground surface with and without piles

for the considered 5 different soil profiles. The acceleration responses at the ground surface for each of the soil profiles in the absence of pile are plotted in Fig. 9, of which the maximum values are compared in Table 4. Results reveal that responses differ for each type of soil profile. In the spectral acceleration responses, case *mm* has the largest values at 3.17Hz and 8.07Hz respectively, and case *pp* has the smallest values for both cases. The maximum accelerations in time domain show that the peak ground acceleration of case *mm* is the largest and that of the case *pp* is the smallest, which difference amounts to 23% (Table 5).

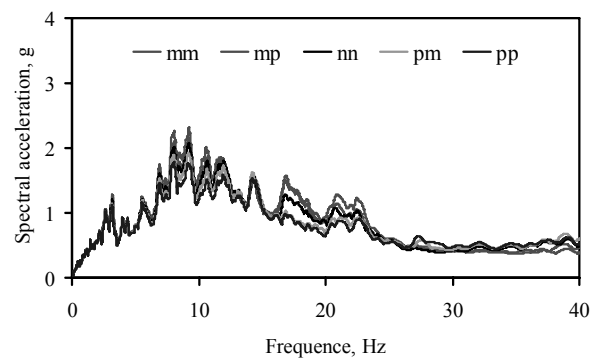
The spectral acceleration responses at the ground surface for model with piles are plotted in Fig. 10, and the peak values of spectral accelerations are listed in Table 6. The responses differ for each type of soil profile

and the response at the frequency of 8.07 Hz shows that the magnitude of case *mm* is 27% larger than that of case *pp*. The variation of peak acceleration in time domain between case *mm* and case *pp* are about 13%. The results (Table 4, 5 versus Table 6, 7) show that the piles decrease the ground acceleration through soil-pile-structure interaction. In the spectral analysis, the amounts of decrease are about 26~20%(3.17Hz) and 20~12%(8.07Hz), which shows that this pile system is more effective in the low frequency range. In the time history analysis, the decrease of the maximum acceleration is about 20%(case *mm*) ~ 12%(case *pp*). One interesting point is that the flat layer (case *nn*) lies always between case *mm* and case *pp*, i.e., case *mm* shows the maximum magnitude and case *pp* shows the minimum magnitude.

Fig. 11 represents the spectral acceleration responses



〈Fig. 9〉 Spectral acceleration at the ground surface for model without piles



〈Fig. 10〉 Spectral acceleration at the ground surface for model with piles

〈Table 4〉 Maximum spectral acceleration at the ground surface for model without piles

| Type | Profile <i>mm</i> | Profile <i>mp</i> | Profile <i>nn</i> | Profile <i>pm</i> | Profile <i>pp</i> |
|---------|-------------------|-------------------|-------------------|-------------------|-------------------|
| 3.17 Hz | 1.753g | 1.740g | 1.652g | 1.422g | 1.409g |
| 8.07 Hz | 2.827g | 2.724g | 2.496g | 2.124g | 2.019g |

〈Table 5〉 Maximum acceleration at the ground surface for model without piles

| Type | Profile <i>mm</i> | Profile <i>mp</i> | Profile <i>nn</i> | Profile <i>pm</i> | Profile <i>pp</i> |
|-----------|-------------------|-------------------|-------------------|-------------------|-------------------|
| Max. acc. | 0.408g | 0.396g | 0.386g | 0.348g | 0.332g |

〈Table 6〉 Maximum spectral acceleration at the ground surface for model with piles

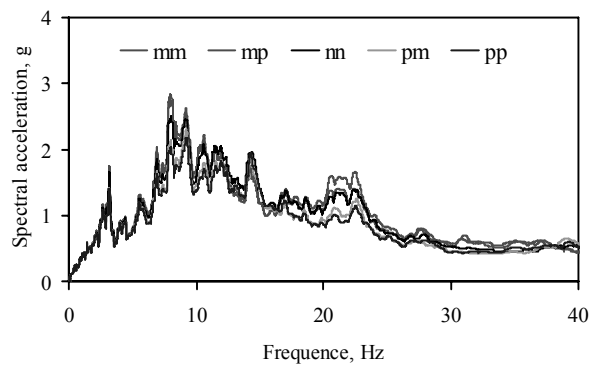
| Type | Profile <i>mm</i> | Profile <i>mp</i> | Profile <i>nn</i> | Profile <i>pm</i> | Profile <i>pp</i> |
|---------|-------------------|-------------------|-------------------|-------------------|-------------------|
| 3.17 Hz | 1.287g | 1.257g | 1.208g | 1.134g | 1.119g |
| 8.07 Hz | 2.250g | 2.093g | 1.995g | 1.879g | 1.765g |

〈Table 7〉 Maximum acceleration at the ground surface for model with piles

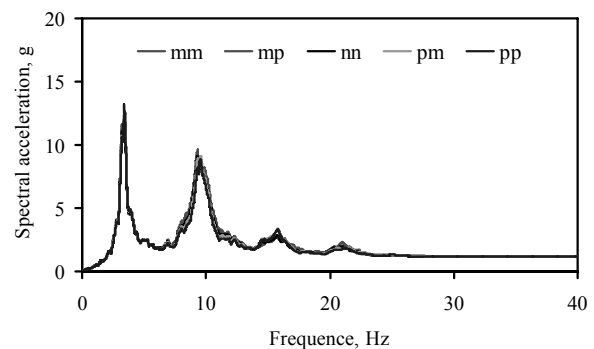
| Type | Profile <i>mm</i> | Profile <i>mp</i> | Profile <i>nn</i> | Profile <i>pm</i> | Profile <i>pp</i> |
|-----------|-------------------|-------------------|-------------------|-------------------|-------------------|
| Max. acc. | 0.328g | 0.312g | 0.300g | 0.305g | 0.292g |

at the top of the structure. The peak values of spectral accelerations at the frequency of 3.21Hz are listed in Table 8. The response at the frequency of 3.21Hz shows that the magnitude of case *mm* is 21% larger than that of case *pp*. The peak acceleration of case *pp* in time domain reaches barely 94.2% of the case *mm* in Table 9. In this example, although the variation of the structural response is small, more significant difference in the structural response may be expected if the amplified frequency range of the soil coincides with frequency of the structure.

We compared above results with the pile case. Fig. 12, Table 10 and 11 presents maximum acceleration at the top of the structure with piles. The shape itself is similar to the case without piles. However, the magnitude decreases are about 15%(case *pp*) ~ 23%(case *mm*).



〈Fig. 11〉 Spectral acceleration at the top of the structure for model without piles



〈Fig. 12〉 Spectral acceleration at the top of the structure for model with piles

〈Table 8〉 Maximum spectral acceleration at the top of the structure for model without piles

| Type | Profile <i>mm</i> | Profile <i>mp</i> | Profile <i>nn</i> | Profile <i>pm</i> | Profile <i>pp</i> |
|---------|-------------------|-------------------|-------------------|-------------------|-------------------|
| 3.21 Hz | 15.152g | 15.001g | 14.361g | 12.643g | 12.408g |

〈Table 9〉 Maximum acceleration at the top of the structure for model without piles

| Type | Profile <i>mm</i> | Profile <i>mp</i> | Profile <i>nn</i> | Profile <i>pm</i> | Profile <i>pp</i> |
|-----------|-------------------|-------------------|-------------------|-------------------|-------------------|
| Max. acc. | 1.274g | 1.267g | 1.267g | 1.216g | 1.200g |

〈Table 10〉 Maximum spectral acceleration at the top of the structure for model with piles

| Type | Profile <i>mm</i> | Profile <i>mp</i> | Profile <i>nn</i> | Profile <i>pm</i> | Profile <i>pp</i> |
|---------|-------------------|-------------------|-------------------|-------------------|-------------------|
| 3.21 Hz | 11.636g | 11.377g | 11.066g | 10.682g | 10.566g |

〈Table 11〉 Maximum acceleration at the top of the structure for model with piles

| Type | Profile <i>mm</i> | Profile <i>mp</i> | Profile <i>nn</i> | Profile <i>pm</i> | Profile <i>pp</i> |
|-----------|-------------------|-------------------|-------------------|-------------------|-------------------|
| Max. acc. | 1.160g | 1.141g | 1.138g | 1.135g | 1.116g |

4. Conclusion

Responses of structures built on soft soils are sensitive to the soil profile and the type of foundation due to soil-structure interaction. Considering the existence of the piles, the response can be more complex and hard to predict accurately without precise calculation. Therefore, the effect of the soil profile and the type of foundation on the structural response should be considered properly in the analysis. However, such consideration is hard to be done due to the limitations of ordinary finite element method in which an element can be endowed only with one material property.

To overcome these difficulties, this paper presented a three-dimensional soil-pile-structure interaction analysis method, which adopts a different numerical integration method that can calculate the stiffness and mass matrices of a finite element with material discontinuity rapidly

and precisely. Applying this method to three-dimensional soil-pile-structure interaction analysis, the dynamic behavior of structures built on soft soil sites with piles were analyzed considering complicated interfaces between materials. Contrary to the ordinary method of mesh arrangement, the proposed method can be easily applied to complex geometries of soil, pile and structure with non-uniform structured mesh, which is very useful because it does not need a fancy mesh generator to catch the surface of material discontinuities in three-dimensional problems. Overall, performance of the proposed analysis shows that it can handle complicated interfaces between materials efficiently.

Analysis results show that dynamic responses of soil-pile-structure system are sensitive to the profile of supporting soil and the existence of piles. The shape variation of the soil layers affects the peak acceleration and the frequency contents of the acceleration for both ground and structure. Piles with enough stiffness decreased the dynamic response in the amount of 20%. The decrease was more dramatic in the low frequency range, which is reasonable because the stiffness of the pile affects soil more directly when the pile is stationary.

Acknowledgement

This work was supported by the Korea Research Foundation Grant funded by the Korean Government (KRF-2008-313-D01049). The present research was conducted by the research fund of Dankook University in 2006.

References

1. Kitiyodom, P., and Matsumoto, T., "A simplified analysis method for piled raft foundations in non-homogeneous soils," *International Journal for Numerical and Analytical Methods in Geomechanics*, Vol. 27, 85-109, 2003.
2. Luco, J.E., Linear soil-structure interaction, *Lawrence Livermore National Lab*, UCRL-15272, 1980.
3. Park, S.H. and Antin, N., "A discontinuous Galerkin method for seismic soil-structure interaction analysis in time domain," *Earthquake Engineering and Structural Dynamics*, Vol. 33, 285-293, 2004.
4. Wang, S., "Coupled boundary and finite elements for dynamic structure-foundation-soil interaction," *Computational Structures*, Vol. 44, 807-812, 1992.
5. Wang, G., Chen, L., and Song, C., "Finite-infinite element for dynamic analysis of axisymmetrically saturated composite foundations," *International Journal for Numerical Methods in Engineering*, Vol. 67, 916-932, 2006.
6. Wolf, J.P., *Dynamic soil-structure-interaction*, Prentice-Hall Inc, 1985.
7. Yang, Z. and Jeremie, B., "Numerical study of group effects for pile groups in," *International Journal for Numerical and Analytical Methods in Geomechanics*, Vol. 27, 1255-1276, 2003.
8. Zohdi, T.I. and Meletis, E.I., "Calculation of hydrogen buildup in the neighborhood of intergranular cracks," *Journal of the Mechanical Behavior of Materials*, Vol. 9, 57-71, 1998.
9. Cook, R.D., Malkus, D.S., and Plesha, M.E., *Concepts and application of finite element method*, 4th ed., John Wiley & Sons Inc, 2001.
10. Park, J.H., Park, J., Park, K.S. and Ok, S.Y., "Analysis of soil-structure interaction considering complicated soil profile," *Lecture Notes in Computer Science*, 4310, 652-659, 2007.
11. Wolf, J.P., *Soil-structure interaction analysis in time domain*, Prentice-Hall Inc, 1988.
12. Hayashi, Y., Tamura, K., Mora, M., and Takahashi, I., "Simulation analysis of buildings damaged in the 1995 Kobe, Japan, earthquake considering soil-structure interaction," *Earthquake Engineering and Structural Dynamics*, Vol. 28, 371-391, 1999.
13. Zhang, Y., Yang, Z., Bielak, J., Contel, J.P. and Elgamal, A., "Treatment of seismic input and boundary conditions in nonlinear seismic analysis of a bridge ground system," *16th ASCE Engineering Mechanics Conference*, 2003.
14. Lysmer, J. and Kuhlemeyer, R.L., "Finite dynamic model for infinite media," *Journal of Engineering Mechanics*, ASCE, 95, 859-877, 1969.
15. Ministry of Construction & Transportation (MOCT), Korean highway bridge design specifications, 2005.
16. Lee, H.S., Lee, J.J., and Jung, D.W., "Analytical Simulation of the Seismic Response of a High-Rise RC Building Model," *Journal of the Earthquake Engineering Society of Korea*, Vol. 12, No. 5, 1-10, 2008.